



A study of binary iron/lithium organometallic complexes as single source precursors to solid state cathode materials for potential Li ion battery application

Jayaprakash Khanderi, Jörg J. Schneider*

Fachbereich Chemie, Anorganische Chemie, Eduard-Zintl-Institut für Anorganische und Physikalische Chemie, Technische Universität Darmstadt, Petersenstraße 18, 64287 Darmstadt, Germany

ARTICLE INFO

Article history:

Received 2 August 2010

Received in revised form 10 January 2011

Accepted 21 January 2011

Available online 4 March 2011

Keywords:

Electrochemistry

Iron

Lithium

Ferrite

Organometallic single source precursor decomposition

ABSTRACT

Solid state and solution phase decomposition of organometallic half sandwich and sandwich complexes of type $[\text{CpFeCODLi} \times \text{DME}]$ **1**, $[\text{CpFeCODLi} \times \text{TMEDA}]$ **2** and $[(\text{Cp})_2\text{FeLi}_2 \times 2 \text{TMEDA}]$ **3** (Cp = cyclopentadienyl, COD = 1,5-cyclooctadiene, DME = dimethoxyethane, TMEDA = tetramethylethylenediamine) derived from ferrocene, yield different kinds of lithium ferrites under oxidative and inert conditions. Thermogravimetry (TG) and TG coupled mass spectrometry of these compounds indicate that the decomposition begins above 170 °C for **1**, 185 °C for **2** and 190 °C for **3** with removal of all the organic ligands. In the absence of oxygen, compounds **1**, **2** and **3** decompose to a mixture of Fe, Fe₃C and Li₂O/Li₂CO₃ at temperatures above 200 °C. Amorphous α -LiFeO₂ is formed in the temperature range of 200–400 °C in the presence of oxygen. Crystalline α -LiFeO₂ is formed only above 400 °C using **1**. Elemental analysis of the LiFeO₂ obtained from **1** indicates a drastic decrease in the carbon and hydrogen content with the increase in the oxidation temperature. XRD reveals the presence of Li₂CO₃ as second phase formed for precursors **1**, **2**, and **3** under oxidative conditions. Solution phase decomposition of **2** and **3** in the absence of oxygen followed by annealing at 600 °C yields Li₂Fe₃O₅, Li₅FeO₄ and Fe₃C depending on the solvent to precursor ratio in contrast to the α -LiFeO₂ phase formed under pure solid state decomposition conditions. However, all lithium ferrites (Li₂Fe₃O₅, Li₅FeO₄) are converted to α -LiFeO₂ when oxidized above 500 °C. The α -LiFeO₂ products were further characterized by IR, XPS, and TEM. Electrochemical analysis of the α -LiFeO₂ was performed, showing a moderate initial capacity of 13 mAh/g.

© 2011 Elsevier B.V. All rights reserved.

1. Introduction

Electrochemically active LiFeO₂ finds application in lithium ion battery as positive and negative electrode material [1–3]. The polymorphs, corrugated layer, goethite and tunnel structured LiFeO₂ are found to be electrochemically active morphologies [4]. LiFeO₂ and other ferrites have been synthesized mainly by ion exchange [1,2,5], microwave assisted [6], solid state [7–9] hydrothermal [10–12] and mechanochemical [13,14] methods using different inorganic Fe and Li salts involving pre-treatments steps of these precursors. Precursor decomposition of Lithium ferric carboxylate complexes with different ligands, Li₃[Fe(L)₆] × H₂O (L = formate, acetate, propionate, butyrate) derived from sol gel type syntheses as well as Li and Fe (acetylacetonate) complexes have also been reported for stoichiometric LiFeO₂ as well as non-stoichiometric Li ferrites [15,16]. The reported methods often need additional annealing at high temperature to form the desired phase and the exact composition of the pre-mixtures is often not known, which

makes the reaction control complicated. Synthetic entries which make use of milder process conditions may have important impact on the composition of the resulting product [10]. Along this direction, we have recently shown that single source molecule $[(\text{COD})_2\text{CoLi} \times (\text{THF})_2]$ can be employed to form electrochemically active LiCoO₂ in the presence of oxygen already at 400 °C [17]. This implies that molecular based precursors are able to deliver active solid state materials with desired functional properties.

Herein we report our studies towards the synthesis, characterization and initial electrochemical performance of electrochemically active LiFeO₂ obtained by decomposition of a family of lithium and iron containing organometallic single source precursors. The decomposition of the organometallic precursors was carried out by solid state as well as solution phase decomposition methods and could circumvent e.g. external mechanical milling to activate precursor components as found for the Li₂CO₃–Fe₂O₃ system [18].

2. Experimental

2.1. Lithium ferrite synthesis

Compounds **1**, **2** and **3** were synthesized as reported [19–22]. Typical solid state and solution phase decompositions were

* Corresponding author. Tel.: +49 6151 163225; fax: +49 6151 163470.

E-mail addresses: joerg64342@web.de, joerg.schneider@ac.chemie.tu-darmstadt.de (J.J. Schneider).

performed by using 80–100 mg of complexes **1**, **2** or **3**. Solid state decomposition experiments under inert atmosphere (Ar flow 200 sccm) were carried out by placing the appropriate compound in an alumina boat and heating to required temperature and holding it for 3 h followed by slow cooling. The precursor compounds were heated to required temperature (200–600 °C) under argon (flow 200 sccm), held for 2 h and then oxidized by passing 10 sccm of oxygen in addition to argon and held for 1 h. The cooling of the products was carried out in argon flow. Depending on the process temperature the final product appeared black to red-brown.

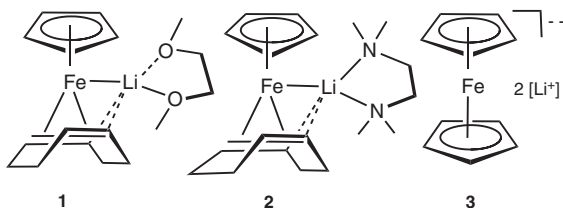
Solution phase decompositions were carried out in trioctylamine (TOA) as solvent (5–10 ml). Compounds **1**, **2** or **3** were mixed with this high boiling solvent and slowly heated to 300–400 °C until weak boiling appears and was maintained for 3 h (heating mantle temperature). The TOA is removed by adding large amount of dry pentane and the suspension is centrifuged repeatedly under air. The resulting product is finally annealed at 600 °C in argon for 3 h (see Scheme 1).

2.2. Sample characterization

Thermogravimetric coupled mass spectrometric (TG-MS) studies were performed using a Netzsch TG209F1 instrument. 10–12 mg of the precursor complex was heated at a heating rate of 10 °C/min. in Helium atmosphere. IR spectroscopic measurements were carried out using a Nicolet FTIR spectrometer with standard KBr pellets. X-ray powder diffraction (XRD) of the samples were performed using StadiP instrument from StadiP, Stoe & Cie GmbH, Darmstadt in Debye–Scherrer mode (flat specimen, transmission mode) with Co K α 1 radiation with a Ge(1 1 1) monochromator. The diffractograms were compared with the reported powder diffraction standards. XPS measurements were performed using ESCA lab 250 (thermo VG scientific) with monochromated Al K α radiation in constant analyzer energy mode (CAE) with a pass energy of 50 eV for all spectra. SEM investigations were performed with Philips XL 30 FEG microscope at 20 keV. HRTEM investigations were carried out using FEI Technai G2 F20 @ 200 kV to determine the size and morphology of the lithium ferrite particles. Samples were prepared in high pure ethanol and dripped on lacy-carbon copper grids.

2.3. Electrochemical measurements

Electrochemical studies were carried out with a multichannel potentiostatic–galvanostatic system VMP (Perkin Elmer Instruments, USA). Swagelok-type cells were assembled in an argon-filled dry box with water and oxygen contents less than 1 ppm. The LiFeO₂ cathodes were prepared by mixing the products of decomposition with carbon (Super P@ Li from TIMCAL) and the carbon from the resulting product, determined by CHN analysis and PVdF (polyvinylidene fluoride) binder in a proportion 70%, 20% and 10%, respectively, and were intimately mixed, ground in an agate mortar with NMP (*N*-methyl pyrrolidone) as solvent. The resulting mixture is pressed onto an Al-mesh (8 mm in diameter, pressure <5 bar). The so prepared cathode is dried at 120 °C



Scheme 1. Molecular structures of mixed Fe/Li half-sandwich complexes **1**, **2** and **3**.

under vacuum for ~5 h. The electrodes contain 3.44 mg of active compound. Lithium metal was used as anode and the electrolyte was 1 M LiPF₆ in EC:DMC 1:2. A glass fiber separator was used between anode and cathode. The cathode was galvanostatically cycled between 2.5 and 4.2 V.

3. Results

The precursors chosen for the present study contain zerovalent iron (for **1** and **2**) as well as divalent iron (**3**). An important aspect is the bonding of lithium in **1**, **2** and **3**. In the case of **1** and **2** lithium is directly bonded to the central zerovalent iron, whereas in the case of **3**, lithium is coordinated to the cyclopentadienyl ring ligand. In the case of **1** and **2** the Fe:Li ratio is 1:1 whereas it is 1:2 for **3**. This offers a different, however constant ratio of the constituent metal ions and allows to tune the phase composition.

3.1. Thermogravimetry of complexes 1, 2 and 3

The thermal characteristics of **1**, **2** and **3** (Fig. 1) have been studied using thermogravimetry (TG) and TG coupled mass spectrometry (TG/MS) in He atmosphere (flow rate 60 ml/min) with a heating rate of 10 °C/min. It can be seen that temperature at which the mass loss occurs for **1** is 60 °C and for **2**, **3** it is approximately 83 °C. The decomposition for all the compounds take place in a two step process followed by progressive weight loss. The initial decomposition step ends at around 160 °C for **1** ($\Delta m = -57.4\%$), 187 °C for **2** ($\Delta m = -59.1\%$) and 190 °C for **3** ($\Delta m = -65.3\%$). The second decomposition step ends around 400 °C for all the three compounds. This indicates, that after removal of the individual organic moieties of **1**, **2** and **3**, a similar solid state reaction occurs, irrespective of the starting compounds composition. The final residues remaining for **1**, **2** and **3** are 40.9% (39.8%), 47.2% (45.3%) and 48.4% (48.4%), respectively (theoretical masses for Fe and Li₂CO₃ for **1**; Fe, Li₂O and Li₂CO₃ for **2**; and Fe₃C, Li₂O for **3** are given in the parenthesis).

3.2. Thermogravimetry coupled mass spectrometry (TG/MS) of complexes 1, 2 and 3

Mass spectra of the gaseous products released from **1** (Fig. 2a and b) and **2** (Fig. 1, ESI) during the thermal cycle indicate fragments due to the decomposition of the organic ligand periphery. Fragments at *m/z* values 16 (CH₄) might account for elimination of methyl moieties from the coordinating ligands and at *m/z* 18 (H₂O) to fragmentation of the oxygenated species in the ligand periphery of **1**. Other primary fragments which evolve during the decomposition of **1** corresponds to DME [*m/z* = 29 (formyl), 42

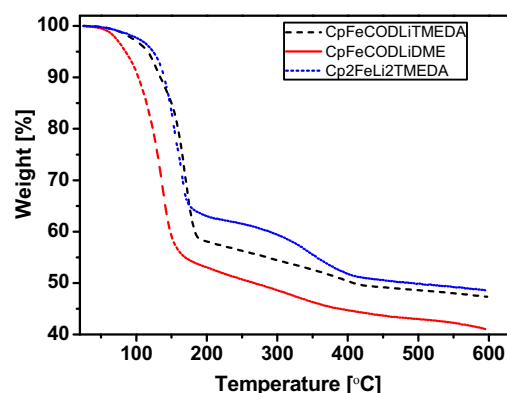


Fig. 1. TG of CpFeCODLiDIME **1** CpFeCODLiTMEDA **2** and (Cp)₂FeLi₂ TMEDA **3** in He atmosphere (flow rate 60 ml/min) and at a heating rate 10 °C/min.

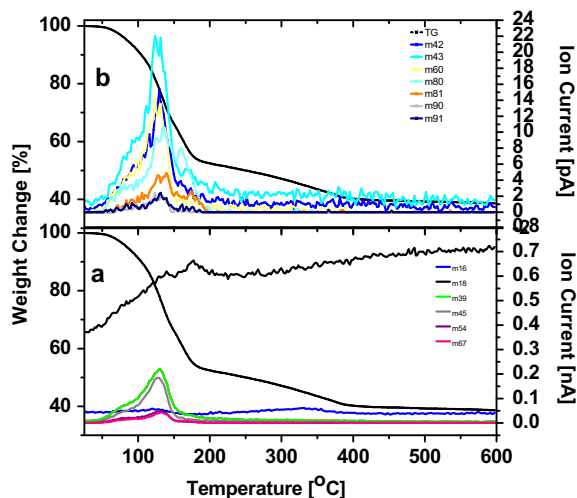


Fig. 2. TG/MS of $[\text{CpFeCODLi} \times \text{DME}] \mathbf{1}$ (a) fragments with nA ion current and (b) fragments with pA ion current.

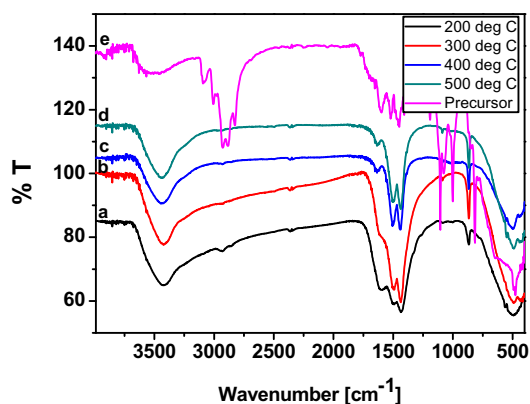


Fig. 3. IR spectra of the product obtained after decomposition of $[\text{CpFeCODLi}] \times \text{DME} \mathbf{1}$ (a) at 200 °C (b) 300 °C (c) 400 °C (d) 500 °C in argon followed by oxygen and (e) that of $\mathbf{1}$.

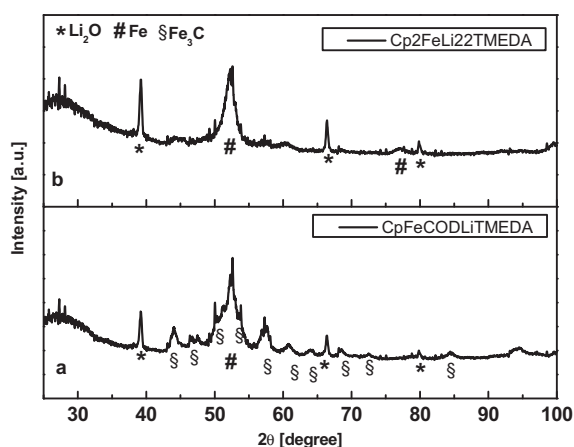


Fig. 4. X-ray powder diffraction pattern of (a) $[\text{CpFeCODLi}] \times \text{TMEDA} \mathbf{2}$ (b) $[(\text{Cp})_2\text{FeLi}_2] \times 2 \text{ TMEDA} \mathbf{3}$, solid state decomposition condition.

(ethenone), 43 (acetyl), 45 (methoxymethyl), 60 (methoxyethyl), 90 (DME)] and TMEDA for $\mathbf{2}$ m/z 43 (*N*-methyl methanimine), 44(methylaminomethyl), 58 (dimethylaminomethyl) as well as for cyclopentadiene (m/z 39 (C_3H_4), 67 (C_5H_8) and 1,5-cyclooctadiene (m/z 39 (C_3H_4), 54 (C_4H_6), 67 (C_5H_8), 80 (C_6H_8)) in the case of complexes $\mathbf{1}$ and $\mathbf{2}$.

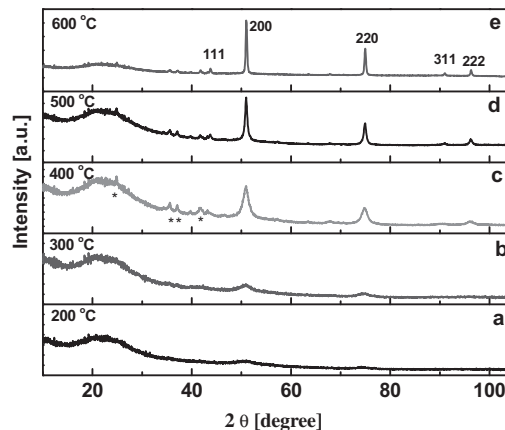


Fig. 5. X-ray diffraction pattern (Co $K\alpha_1$) of the LiFeO_2 derived from in the presence of oxygen at (a) 200, (b) 300, (c) 400, (d) 500 and (e) 600 °C (*corresponds to Li_2CO_3).

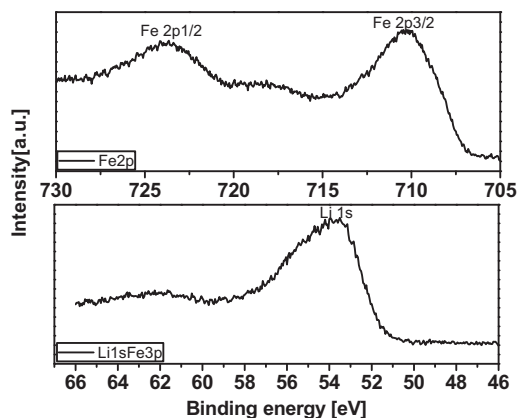


Fig. 6. X-ray photoelectron spectra of LiFeO_2 (a) Fe 2p region (b) Li_{1s} and Fe_{3p} region.

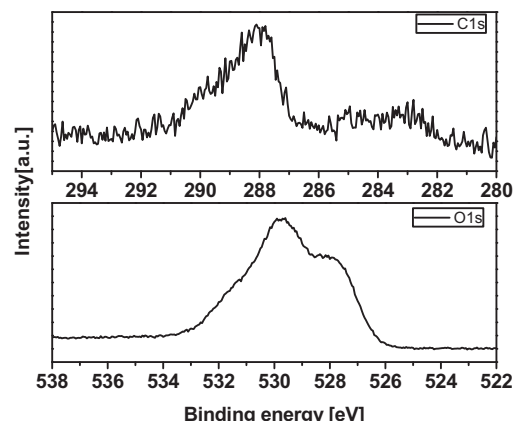


Fig. 7. X-ray photoelectron spectra (a) C_{1s} (b) O_{1s} of LiFeO_2 obtained from $\mathbf{1}$.

3.3. Infrared spectroscopy of $\mathbf{1}$, $\mathbf{2}$, and $\mathbf{3}$

IR spectra of precursor and product obtained after decomposition of $\mathbf{1}$ at different temperatures in the presence of argon followed by oxygen is shown in Fig. 3. Comparison of the spectrum of molecular complex of $\mathbf{1}$ with the decomposition product of $\mathbf{1}$ obtained at 200 °C reveals that weak absorption bands at 2936 and 2853 cm^{-1} are present. These can be accounted for the C–H stretching vibrations of methylene and/or carbene groups resulting

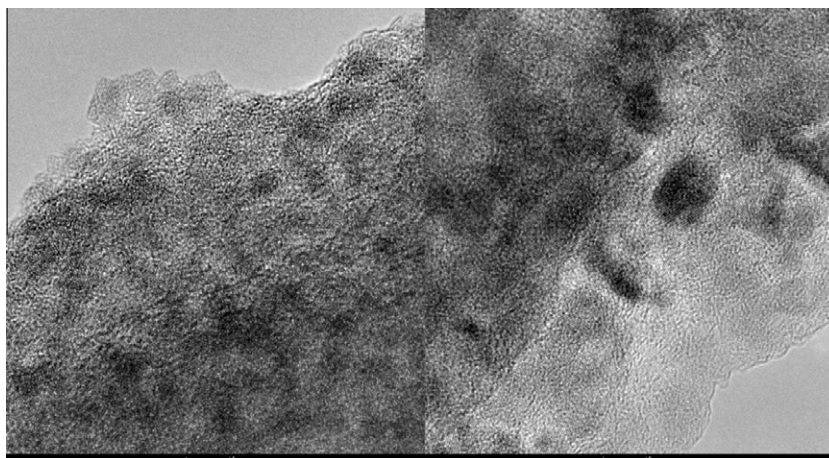


Fig. 8. TEM (left) and HRTEM (right) of the LiFeO_2 powder obtained from thermal decomposition of precursor $[\text{CpFeCODLi}] \times \text{DME } \mathbf{1}$ at temperature of 200°C .

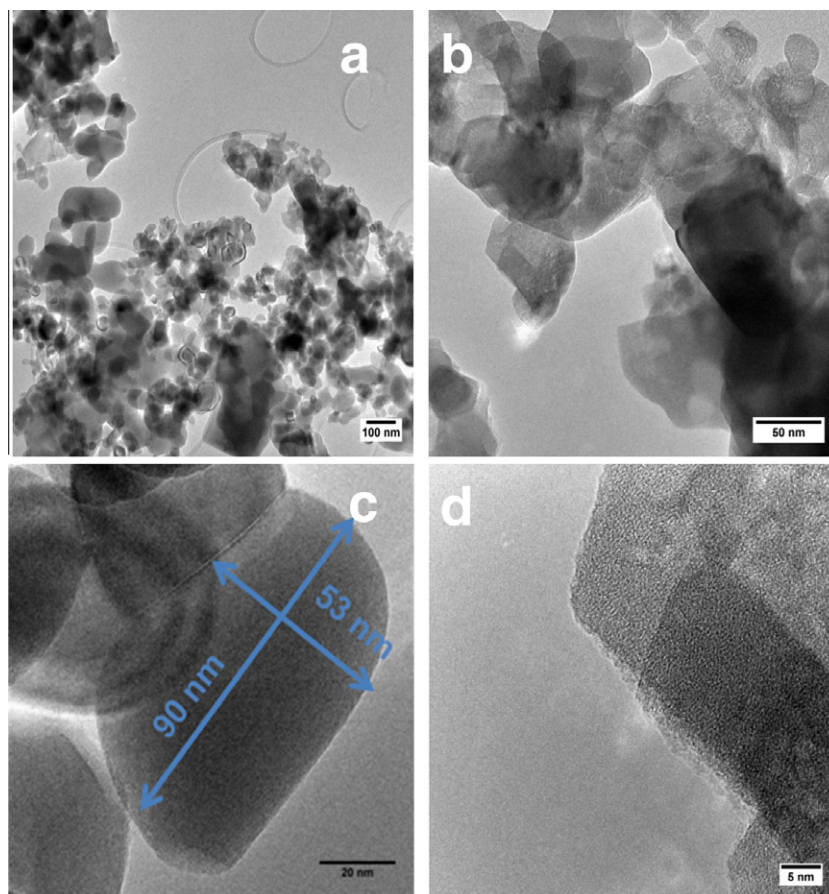


Fig. 9. TEM LiFeO_2 powder obtained from thermal decomposition of precursor $[\text{CpFeCODLi}] \times \text{DME } \mathbf{1}$ at 600°C (a) particle of in the size range of $40\text{--}90\text{ nm}$ and $150\text{--}300\text{ nm}$, (b) showing irregular shape and flaky morphology (c) image indicating typical dimension of the particle (d) HRTEM of the LiFeO_2 , where disordered structure with in the particle can be seen.

from the decomposition of the cycloalkene ligands of **1**, indicating that the majority of the organic ligands have been removed already at 200°C . The remaining decomposition product thus obtained in the temperature range between 200 and 500°C show absorptions at $1495\text{--}1503\text{ cm}^{-1}$, 1430 cm^{-1} and 870 cm^{-1} corresponding to Li_2CO_3 [23] and those at $1600\text{--}1630\text{ cm}^{-1}$ account for carbonaceous residues. Importantly it can be concluded that all decomposition products obtained in the decomposition temperature range between 200 and 500°C contain Li_2CO_3 .

3.4. X-ray diffraction (XRD)

3.4.1. Solid state decomposition of precursors **2** and **3** in the absence of oxygen

Precursors **2** and **3** were decomposed in the absence of solvent and oxygen, at a temperature of 600°C under an argon atmosphere. Precursor **2** decomposes to Fe , Fe_3C and Li_2O (Fig. 4a) whereas **3** gives Fe and Li_2O (Fig. 4b). This indicates that during the decomposition the reactivity of the components and the amount of carbon

containing species determines the type of solid state product formed, accounting for different carbon rich and carbon free phases.

3.4.2. Solution phase decomposition under absence of oxygen

The solution phase decomposition of **2** and **3** results in different lithium ferrite solid materials. The formation of these ferrites is dependent upon the solvent to precursor ratio. When the amount of the precursor in trioctylamine (TOA) is low, both, **2** and **3** yield $\text{Li}_2\text{Fe}_3\text{O}_5$ with varying amount of Li_2CO_3 for **2** (similar results for **3**). When the amount of the precursor is increased in the same solvent TOA, **3** however, gives Fe_3C and Li_5FeO_4 . In all cases the as synthesized product is tempered at 600 °C to give the final crystalline product. The primary decomposition products obtained before the tempering step show only the presence of Fe [ESI, Fig. 2], pointing towards the fact that during the tempering step the amorphous lithium compounds react further with iron or oxides of iron formed in the decomposition process, giving rise to various type of ferrites. This fact is studied in the upcoming Section 3.4.3.

3.4.3. Solid state decomposition of **1** under oxygen

The decomposition of **1** in solid state and in solution under oxygen has been carried out. The experiments were performed by heating **1** in inert atmosphere at 200–600 °C followed by passing oxygen over the so prepared material at respective temperatures. The product obtained in the solution state decomposition ($\text{Li}_2\text{Fe}_3\text{O}_5$ and Li_5FeO_4) was heated in air. Fig. 6 shows the XRD of products obtained from decomposition of **1** at 200–600 °C. First, amorphous $\alpha\text{-LiFeO}_2$ is observed at 200 °C. As the temperature is increased, the initially formed $\alpha\text{-LiFeO}_2$ converts to a crystalline phase. Li_2CO_3 formation was also observed above 400 °C. The products of the solution phase decomposition, $\text{Li}_2\text{Fe}_3\text{O}_5$ or Li_5FeO_4 , obtained after annealing, as well as the as synthesized product from the solution phase decomposition were converted to $\alpha\text{-LiFeO}_2$, with varying amounts of Li_2CO_3 when heated to 500 °C or above in air/oxygen.

The product obtained at 200 °C was studied by XRD (Fig. 5). Between 400 and 550 °C a drastic structural change occurred. At 550 °C however, the [2 2 0] diffraction peak splits into two peaks at 2θ 50.2° and 50.6°. The peak at 2θ 50.6°, increases in intensity with temperature, indicating crystallization and a close structural relationship between the products obtained at low and higher temperature.

3.5. X-ray photoelectron spectroscopy (XPS) obtained from **1**

XPS spectra of Fe_{2p} and $\text{Li}_{1s}/\text{Fe}_{3p}$ for LiFeO_2 synthesized from **1** at a temperature of 600 °C are shown in Fig. 6. The signals for $\text{Fe } 2p_{3/2}$ and $\text{Fe } 2p_{1/2}$ are observed at 710.3 eV and 723.8 eV, respectively, and a good indication for the presence of Fe(II) species in addition to Fe(III) [24]. The BE of $\text{Li}_{1s}/\text{Fe}_{3p}$ overlap each other and appear at approximately 55.6 eV with a shoulder at 53.7 eV. The lower BE shoulder can be assigned to Fe(II)/Fe(III) state, present in the LiFeO_2 product. The higher BE value overlaps both for 3p Fe and 1s Li.

The high resolution XPS spectra of the C_{1s} and O_{1s} excitations of LiFeO_2 obtained from **1** at 600 °C are depicted in Fig. 7. The C_{1s} spectrum shows low intensity signals at 283.0 eV, 284.3 eV and 288.1 eV, and an additional shoulder at 289.7 eV. The signal at 283.0 eV can be accounted for carbon such as in the carbide Fe_3C . The peak at BE 284.3 eV shows that at 600 °C a small amount of the graphitic carbon is still left in the material. The higher BE peak at 288.1 can be accounted for carbon in a polymeric state. The shoulder at BE 289.7 eV corresponds to carbon resulting from carbonate ion, due to the minor presence Li_2CO_3 .

The O_{1s} signals appears at 528.4 eV, 529.7 eV and 531.4 eV (Fig. 7b). The signal at a BE of 528.4 eV can be accounted for Fe(II) and Fe(III) [25]. The peak component at 529.7 eV corresponds to O^{2-} ions in the crystal structure of LiFeO_2 [26]. The second peak

at 531.4 eV can be assigned to oxygen associated with the organo-metallic precursor **1** [27].

These combined findings show that there are different decomposition reactions occurring during high temperature decomposition of **1** at 600 °C. No clear decomposition pathway can be drawn from these findings.

3.6. Transmission electron microscopy (TEM)

High resolution (HR)TEM micrographs of the LiFeO_2 synthesized under oxidative conditions at 200 °C are depicted in Fig. 8a and b. 2–4 nm sized particles are found to be embedded inside an amorphous shell. The particles are of a rounded morphology and show a uniform size distribution.

TEM micrographs of LiFeO_2 synthesized under oxidative conditions at 600 °C are shown in the Fig. 9a–d. It can be observed that the LiFeO_2 material produced at 600 °C is comprised of particle in size range 40–90 nm as well as bigger ones being 150–300 nm. Overall size dimensions of a typical LiFeO_2 are shown in Fig. 9c. A HRTEM image reveal the low crystallinity of the product well in accordance with previous investigations on $\alpha\text{-LiFeO}_2$ [28]. This finding already indicates that the electrochemical activity of the so formed lithium ferrite could not be expected to be extraordinary high (see Section 3.7)

3.7. Electrochemical analysis

Electrochemical analysis of the LiFeO_2 obtained from precursor **1** at 600 °C is shown in Fig. 10. The capacity variation with the voltage is shown in Fig. 11a. It can be observed that only in the first cycle lithium can be extracted, but due to the drastic change in the structure of the delithiated LiFeO_2 the further intercalation becomes hindered. The discharge capacity decreases rapidly with cycle number indicating the instability of the thus formed LiFeO_2 for electrochemical cycles (Fig. 10b).

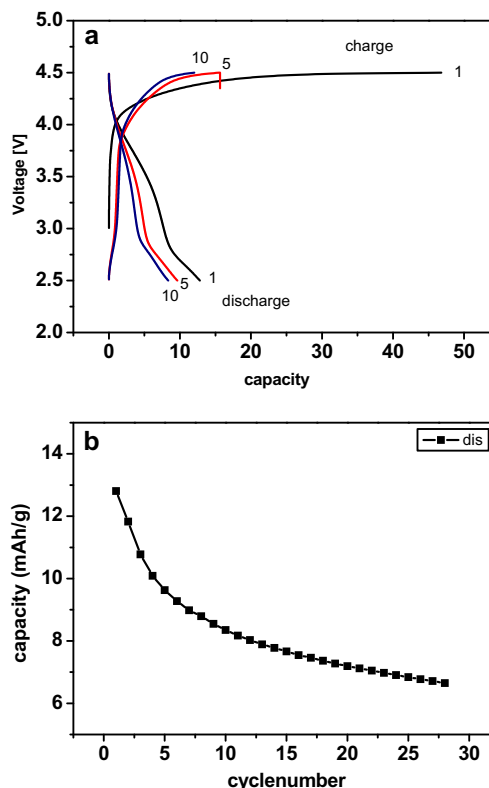


Fig. 10. (a) Capacity variation during charge and discharge cycles and (b) variation of discharge capacity of LiFeO_2 synthesized at 600 °C against cycle number.

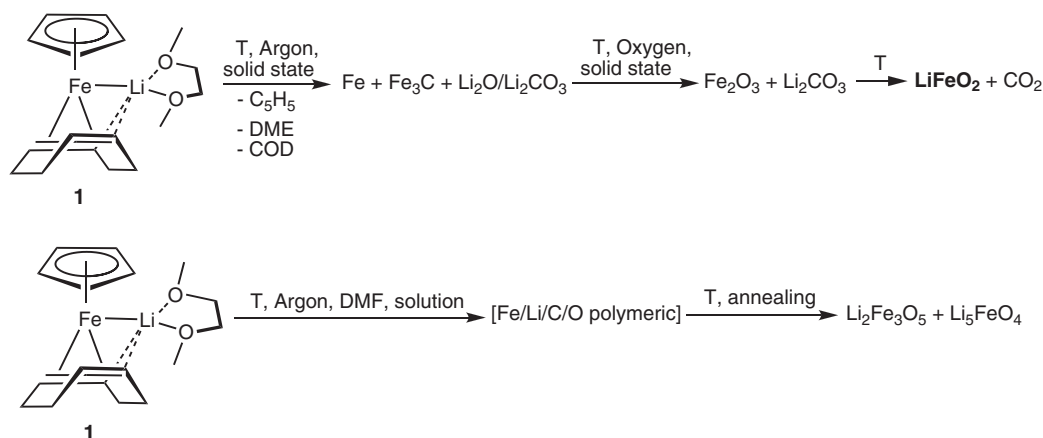


Fig. 11. Reaction scheme for the decomposition and further reactions leading to the formation LiFeO₂ from compound 1.

4. Discussion

The solid state decomposition of the precursors **1–3** in the absence of oxygen results in the formation of iron, Fe₃C, and Li₂O/Li₂CO₃, the latter formed reaction of Li with traces of oxygen and CO₂/H₂O as indicated by XRD, IR and TG. TG/MS shows that the organic ligand sphere for **1–3** is eliminated already below 200 °C. TEM of the product obtained at 200 °C shows particle dimensions of 2–4 nm are embedded inside an amorphous matrix. Fe(II) and Fe(III) is formed during the initial decomposition starting from Fe(0) in the precursors and form the mixed iron oxide, which further reacts with Li₂CO₃ resulting in formation of LiFeO₂.

In the case of the solution phase decomposition, ferrites such as Li₂Fe₃O₅ or Li₅FeO₄ are formed indicating a different decomposition pathway compared to the solid state. The decomposition reactions based on the spectroscopic and microscopic findings resulting in the formation of LiFeO₂ from **1**, are depicted in Fig. 11.

5. Conclusions

Lithium containing ferrocene derivatives of the type [(Cp)Fe(COD)Li × (L)] (L = DME, TMEDA) and [(Cp)₂FeLi₂ × 2 L] (L = TMEDA) are suitable single source precursors for the preparation of lithium ferrites of various compositions. These organometallic compounds can be decomposed in the solid state as well as in solution to give solid state ferrite materials. The decomposition in inert atmosphere leads to the formation of a mixture Fe, Fe₃C and Li₂O/Li₂CO₃ as precursor material with the complete removal of all organic ligands. These initially formed components react further under oxidative conditions to form LiFeO₂ by reaction of iron oxide and Li₂O/Li₂CO₃. The so formed amorphous LiFeO₂ crystallizes as the temperature is further increased. HRTEM of the final product obtained at 600 °C reveals no crystalline order. In the case of solution phase decomposition, various fragments containing lithium and iron might react in a more complicated route leading to the formation of other ferrites. The electrochemical test of the α-LiFeO₂ formed via the solid state decomposition route shows an initial capacity of 13 mAh/g with a rapid decrease in capacity. To conclude, lithium containing ferrocene derivative are promising precursors for the synthesis of lithium ferrites.

Acknowledgments

Our work is supported through the Deutsche Forschungsgemeinschaft (DFG). We acknowledge Dr. Rudolf C. Hoffmann (TG/MS), Dr. Alexander Issannin (XPS), Dr. Kathrin Hofmann, Dr. Gerhard

Cordier (XRD) and Dr. Jörg Engstler (TEM), for technical assistance. We thank the Ernst-Ruska-Zentrum, Jülich (Prof. H. Meyer, Dr. L. Houben, Dr. A. Lysberg) for making TEM studies possible (under Project ERC1-TUD).

Appendix A. Supplementary data

Supplementary data associated with this article can be found, in the online version, at doi:10.1016/j.ica.2011.01.074.

References

- [1] A.R. Armstrong, D.W. Tee, *J. Am. Chem. Soc.* 130 (2008) 3554.
- [2] P.P. Prosin, M. Carewska, S. Loreti, C. Minarini, S. Passerini, *Int. J. Inorg. Mater.* (2002) 365.
- [3] M. Holzapfel, R. Schreiner, A. Ott, *Electrochem. Acta* 46 (2001) 1063.
- [4] Y. Sakurai, H. Arai, J.-I. Yamaki, *Solid State Ionics* 113–115 (1998) 29.
- [5] T. Shirane, R. Kanno, Y. Kawamoto, Y. Takade, M. Takano, T. Kamiyama, F. Izumi, *Solid State Ionics* 79 (1995) 227.
- [6] A.S. Vanetsev, V.K. Ivanov, Y.D. Tretyakov, *Doklady Chem.* 387 (2002) 332.
- [7] G.A. El-Shobaky, A.A. Ibrahim, *Thermochem. Acta* 118 (1987) 151.
- [8] V. Berbenni, A. Marini, G. Bruni, R. Riccardi, *Thermochem. Acta* 346 (2000) 115.
- [9] Y.S. Lee, C.S. Yoon, Y.K. Sun, K. Kobayakawa, Y. Sato, *Electrochem. Commun.* 4 (2002) 727.
- [10] M. Tabuchi, K. Ado, H. Sakaebe, C. Masquelier, H. Kageyama, O. Makamura, *Solid State Ionics* 79 (1995) 220.
- [11] M. Tabuchi, C. Masquelier, T. Takeuchi, K. Ado, I. Matsubara, T. Shirane, R. Kanno, S. Tsutsui, S. Nasu, H. Sakaebe, H. Kageyama, O. Makamura, *Solid State Ionics* 90 (1996) 129.
- [12] C. Barriga, V. Barron, R. Gancedo, M. Gracia, J. Morales, J.L. Tirado, J. Torrent, *J. Solid State Chem.* 77 (1988) 132.
- [13] J.M. Fernandez-Rodriguez, J. Morales, J.L. Tirado, *J. Mater. Sci. Lett.* 6 (1987) 223.
- [14] J.M. Fernandez-Rodriguez, J. Morales, J.L. Tirado, *J. Mater. Sci.* 23 (1988) 2971.
- [15] B.S. Randhawa, H.S. Dosanjh, N. Kumar, *J. Radioanal. Nucl. Chem.* 274 (2007) 581.
- [16] M. Vucinic-Vasic, B. Antic, J. Blanus, S. Rakic, A. Kremenovic, A.S. Nikolic, A. Kapor, *Appl. Phys. A* 82 (2006) 49.
- [17] J. Khanderi, J.J. Schneider, *Eur. J. Inorg. Chem.* (2010) 4591–4594.
- [18] V. Berbenni, A. Marini, P. Matteazzi, R. Ricceri, N.J. Welham, *J. Eur. Ceram. Soc.* 23 (2003) 527.
- [19] K. Jonas, L. Schieferstein, C. Krüger, Y.-H. Tsay, *Angew. Chem.* 91 (1979) 590.
- [20] K. Jonas, L. Schieferstein, C. Krüger, *Angew. Chem., Int. Ed.* 18 (1979) 549.
- [21] D. Guillaneux, H.B. Kagan, *J. Org. Chem.* 60 (1995) 2502.
- [22] A. Fürstner, K. Majima, R. Martin, H. Krause, E. Kattinig, R. Goddard, C.W. Lehmann, *J. Am. Chem. Soc.* 130 (2008) 1992.
- [23] P. Pasierb, S. Komornicki, M. Rokita, M. Rekas, *J. Mol. Struct.* 596 (2001) 151.
- [24] G.C. Allen, M.T. Curtis, A.J. Hooper, P.M. Tucker, *J. Chem. Soc., Dalton Trans.* (1974) 1525.
- [25] R.M.T. Sanchez, E.M. Curt, C. Volzone, R.C. Mercader, A.L. Cavalieri, *Mater. Res. Bull.* 25 (1990) 553.
- [26] T. Miyazaki, T. Doi, M. Kato, T. Miyake, I. Matsuura, *Appl. Surf. Sci.* 121–122 (1997) 492.
- [27] S. Srivastava, S. Badrinarayanan, A.J. Mukhedkar, *Polyhedron* 4 (1985) 409.
- [28] N. Tanaka, J.M. Cowley, *Ultramicroscopy* 17 (1985) 365.